Spectroscopic investigation of fs laser-induced defects in polymer and crystal media

Kallepalli Lakshmi Narayana Deepak[1, 2], Soma Venugopal Rao, Desai Narayana Rao[3]

[1] Aix Marseille Universite, CNRS, LP3 UMR 7341,13288 Marseille, France.
Email : dkln1982@gmail.com, kallepalli@lp3.univ-mrs.fr
[2] School of Physics, [3] Advanced Centre of Research in High Energy Materials
University of Hyderabad, Hyderabad 500046, India. Phone: 91 040 23134335.
Author for correspondence: dnrsp@uohyd.ernet.in

ABSTRACT

We investigated formation of defects in four polymers namely Poly (methylmethacrylate) [PMMA], Poly dimethylsiloxane [PDMS], Polystyrene [PS], and Polyvinyl alcohol [PVA] and crystal media such as Lithium Niobate [$LiNbO_3$]. Spectroscopic studies of the femtosecond (fs) laser modified regions were systematically performed after fabricating several gratings and micro-channels. We observed emission from the fs laser modified regions of these polymers when excited at different wavelengths. Pristine polymers are not paramagnetic, but exhibited paramagnetic behavior upon fs irradiation. $LiNbO_3$ (LNB) crystal has not shown any defect formation upon laser irradiation. Confocal micro-Raman studies were also performed to establish the formation of defects.

Keywords: Free radicals, emission, confocal micro-Raman, femtosecond laser direct writing, defects.

1. INTRODUCTION

Femtosecond laser direct writing has been successfully implemented to fabricate three dimensional structures inside various transparent materials over the last decade. Since the absorption is strongly nonlinear, these modifications can be localized within the focal volume, and inside the bulk material, leaving the surrounding region unaffected [1-2]. This interaction of femtosecond laser pulses with dielectric materials has significance both for fundamental knowledge of basic ionization processes and for laser technology and industrial applications [3-7]. In dielectric materials like glasses and polymers, the conduction band is empty and the matter is transparent to the laser light. Due to nonlinear ionization processes the electrons from the valence band are transferred to the conduction band by photo–ionization process which depends on the laser field and material [8]. The seed electrons thus excited into the conduction band absorb the laser energy and further if the kinetic energy of the conduction electrons exceeds a critical value, they can further ionize other bound electrons in the valence band inducing the avalanche ionization process. The ionized dielectric medium starts to behave like a metal with a time varying electron density in the conduction band. The deposited laser energy is then transferred to the lattice, and thermo-mechanical relaxation and ejection of matter processes occur depending of the amount of absorbed laser energy density. In the present study we present defect formation due to photo-ionization process and show some of the applications that can be realized.

2. EXPERIMENTAL SECTION

For our experiments, we purchased PMMA sheet from Goodfellow, USA. PDMS was homemade. PS was purchased from Goodfellow, UK. PVA thin films were prepared by dissolving 8.56 grams of PVA beads in 100 ml of water and then with a spin coating technique. Thin films of PS are made by preparing the PS solution first. Solution of PS was prepared by mixing 1 gram of polystyrene beads (ACROS) in 8 ml toluene and stirred for 48 hours for complete miscibility. Initially, we fabricated several structures in polymers PMMA, PDMS, PS and PVA. We used x-cut $LiNbO_3$ (LNB) crystal for our experiments. Before microfabrication experiments carried out, these samples were sonicated in distilled water to remove unwanted dust. Microstructures, and 2-dimensioal grids (for ESR analysis) are fabricated using a Ti: sapphire oscillator amplifier system operating at a wavelength of 800 nm delivering ~100 fs pulses, ~1 mJ output

Laser-Induced Damage in Optical Materials: 2012, edited by Gregory J. Exarhos, Vitaly E. Gruzdev, Joseph A. Menapace, Detlev Ristau, M J Soileau, Proc. of SPIE Vol. 8530
853004 · © 2012 SPIE · CCC code: 0277-786/12/$18 · doi: 10.1117/12.975812

energy pulses with a repetition rate of 1 kHz. The near-transform nature of the pulses was confirmed from the time-bandwidth product. Three translational stages (Newport) were arranged three dimensionally to translate the sample in X, Y, and Z directions. Laser energy was varied using the combination of half wave plate and a polarizer. We have used 40X (Numerical Aperture (NA) of 0.65) and 20X (NA of 0.4) microscope objectives in our experiments for focusing. Figure 1 shows the schematic of fs laser direct writing set up that we used for our irradiation experiments. HWP and BP are half wave plate and polarizer to vary the laser energy. M1-M3 are the mirrors used to vertically focus the laser beam into microscope objective MO as shown in the picture. Also we used CCD camera next to XYZ stage to view the focused spot which helped us to fabricate structure either on or inside the surface of the substrates.

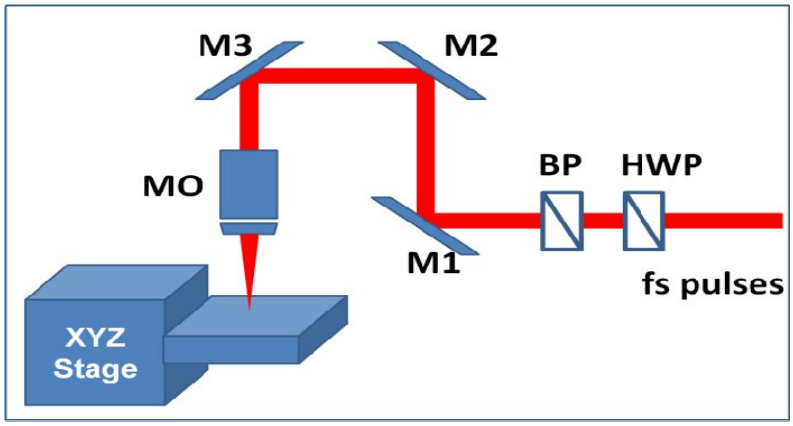

Figure 1. Fs laser direct writing setup.

3. THRESHOLD INTENSITY, THERMAL DIFFUSION LENGTH, AND KELDYSH PARAMETER CALCULATIONS

Here we present threshold intensity required to produce laser damage for different polymers and LNB crystal. The threshold intensity required for laser damage in different polymers investigated are presented herein. We use the equation (1) to find out the threshold intensity for laser damage at different pulse widths from ns to fs regime. The formula to calculate the threshold intensity is given by

$$I_{th} = n\varepsilon_0 c\left\langle E^2 \right\rangle = 2n\varepsilon_0 c \frac{Wm}{fe^2\tau T_p} \ln(N_{th}/N_0) \qquad (1)$$

I_{th} is the threshold intensity for laser damage. $\ln(N_{th}/N_0)$ can be taken as 30. W is the ionization potential for which we considered the bandgaps for various polymers. All other terms in the equation have their usual meanings taken from reference 9. The bandgap of PMMA is 4.58 eV, PDMS is 2.84 eV, PS is 4.54 eV, and PVA is 2.4 eV [10-14]. LNB crystal has band gap of 3.75 eV [15-16] which is in between the bandgap of PDMS and PS. Here, we present our results in table 1. From table 1, we see that the threshold intensity for producing laser damage increases with shortening the pulse as it is evident from the formula (1).

In the calculations, we have assumed f≈0.01 [9]. f is defined as the fraction of the absorbed energy that leads to ionization. The value of f is different for different materials though we considered it to be equal to 0.01. τ is defined as the mean time between collisions which is taken as 10^{-15}s [9]. Under several such assumptions as referenced in 9, we calculated the threshold intensities for different pulse widths in these polymers. We used 100 fs pulses throughout our irradiation experiments with different polymers and LNB crystal. The order of magnitude is sub PW/cm^2 for almost all polymers that are investigated. Since fs pulsed lasers can produce PW/cm^2 intensities, micromachining with fs lasers is preferable. Since the bandgaps of PMMA and PS are nearly equal, we see from table 1 that they both have same I_{th}.

Results obtained with 100 fs pulses are highlighted red in color. In case of LNB also, we obtained similar results with same magnitude as its band gap is in between PDMS and PS.

Table 1. Threshold intensity for laser damage for different pulse durations in different polymers investigated.

S. No.	T_p	I_{th}			
		PMMA	PDMS	PS	PVA
1	1 fs	41.5 PW/cm^2	25.73 PW/cm^2	41.13 PW/cm^2	21.74 PW/cm^2
2	10 fs	4.2 PW/cm^2	2.573 PW/cm^2	4.11 PW/cm^2	2.174 PW/cm^2
3	**100 fs**	**0.414 PW/cm^2**	**0.26 PW/cm^2**	**0.411 PW/cm^2**	**0.22 PW/cm^2**
4	1 ps	41.49 TW/cm^2	25.73 TW/cm^2	41.13 TW/cm^2	21.74 TW/cm^2
5	10 ps	4.15 TW/cm^2	2.573 TW/cm^2	4.11 TW/cm^2	2.174 TW/cm^2
6	100 ps	0.415 TW/cm^2	0.26 TW/cm^2	0.411 TW/cm^2	0.22 TW/cm^2
7	1 ns	41.49 GW/cm^2	25.73 GW/cm^2	41.13 GW/cm^2	21.74 GW/cm^2
8	10 ns	4.15 GW/cm^2	2.573 GW/cm^2	4.11 GW/cm^2	2.174 GW/cm^2
9	100 ns	0.415 GW/cm^2	0.26 GW/cm^2	0.411 GW/cm^2	0.22 GW/cm^2

We calculated the thermal diffusion lengths for polymers and the dielectric materials in general. Since we could not get diffusion constants for few materials, we have taken the usual value for any dielectric system and then calculated thermal diffusion lengths for different pulse widths. The thermal diffusion length is given by

$$L = \left(DT_p\right)^{1/2} \qquad (2)$$

where D is the diffusion constant, L is thermal diffusion length and T_p is the pulse duration. The D values for PMMA and PS are taken as 0.11 and 0.525 mm^2/s [17-20]. The values of D typically will be of the order of 10^{-3} cm^2/s for dielectrics. Table 2 shows the diffusion lengths for different materials at different pulse durations. We used 100 fs pulses and the calculated thermal diffusion lengths which are indicated in red color of table 2. From table 2, it is noticed that thermal diffusion length increases with the increase in pulse duration for almost all materials. Thus, thermal effects are almost negligible for fs pulses. It is for this reason; fs pulses are preferred over ns, and ps pulses for micro structuring different materials. Figure 2 shows the plot obtained between thermal diffusion lengths with pulse duration for different materials. Since the thermal diffusion lengths obtained for ps, and fs pulses are very less and nearly zero and cannot be seen in the graph, we have taken log of the thermal diffusion length on the Y axis.

Table 2. Thermal diffusion lengths for different materials at different pulse durations.

S. No.	T_p	L(nm)		
		PMMA	PS	Dielectrics
1	1 fs	0.01	0.023	0.01
2	10 fs	0.033	0.073	0.032
3	**100 fs**	**0.105**	**0.23**	**0.1**
4	1 ps	0.3	0.725	0.32
5	10 ps	1.05	2.3	1
6	100 ps	3.32	7.25	3.2
7	1 ns	10.5	23	10
8	10 ns	33	72.5	32
9	100 ns	105	230	100

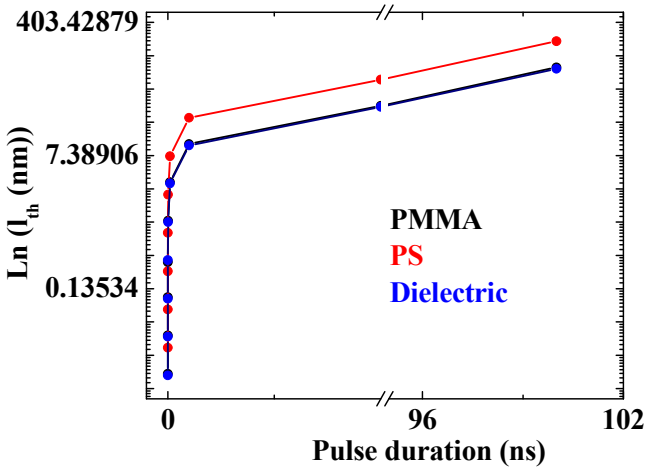

Figure 2. Logarithm of thermal diffusion length with pulse duration.

In these calculations the role of repetition rate of the laser is neglected. There could be multiple irradiations at the same irradiated spot if repetition rate of the laser is high. In the calculations of thermal diffusion length also, we have neglected the intensity of the laser to arrive at the equation (2) as explained in the reference 9. Also as these materials have large bandgaps, one 800 nm (1.55 eV) photon cannot excite electrons from the valence band to conduction band . Here, we show the Keldysh parameter calculations used to assess the ionization process which is dominant when laser pulses interact with different materials. Most of the transparent polymers are wide bandgap materials. Their bandgap ranges from 2.2 to 2.4 eV for chalcogenide glasses and up to 8.8 eV for sapphire that ensures the transparency in the visible or near infrared spectral range at low intensity [21]. Most of the transparent polymers are also wide bandgap materials. The Keldysh parameter (γ) which provides information about the dominant mechanism is defined as

$$\gamma = \frac{\omega}{e}\left[\frac{mc\varepsilon_0 E_g}{I}\right]^{1/2} \qquad (3)$$

m, e are the reduced mass and charge of the electron, I is the intensity, ω is the laser frequency, ε_0 is the permittivity of free space, E_g is the bandgap of the material, n is the refractive index of the material, and c is the velocity of light. Multiphoton ionization is dominant in case of γ >1.5, and tunneling ionization is favored in case of γ <1.5. If γ =1.5, then both ionizations are dominant [9, 22-24]. The energy of an 800 nm photon corresponds to 1.55 eV while the optical band gap of pure PMMA is 4.58 eV which implies that the nonlinear process involving at least three photons is responsible for structural modification at the focal volume [10]. The bandgaps for PS, PVA, and PDMS are 4.3-4.54 eV, 2.92 eV, 2-2.84 [10-14] respectively. The information of bandgap suggests that multiphoton ionization is responsible for the modification of polymers as bandgap energies are more than 800 nm photon energy. But the calculation of Keldysh parameter suggested that the tunneling ionization is mostly responsible for the modification process. For this, we calculated peak intensities (I), which is the peak power (P) divided by area of the focused spot. Area of the focused spot is given by

$$A = \pi r^2 \qquad (4)$$

where r is the radius of the spot. For microfabrication experiments carried out with 40X objective with numerical aperture (NA) 0.65, the spot size is calculated as

$$d = \frac{1.22\lambda}{NA} \qquad (5)$$

where λ is wavelength of the laser used (800 nm). The spot sizes thus estimated are 1.55 and 2.4 μm respectively for 40X and 20X microscope objectives. The peak power further is given by energy of the pulse multiplied by frequency of the laser which is 1 KHz (repetition rate). In our experiments with four different polymers PMMA, PDMS, PS and PVA we varied the energy from 150 μJ-460 nJ. Figure 3 shows the plot of Keldysh parameter with peak intensity for different polymers. The Keldysh parameter, less than 1.5, shows that the main mechanism responsible for modification is tunneling ionization. For polymers investigated in our experiments, the tunneling ionization is shown to be mainly responsible for modification process involved. We extended our analysis to evaluate where Keldysh parameter nears 1.5. From the plot, we found that Keldysh parameter nears and becomes larger than 1.5 for pulse energies of 30 nJ. Thus for structures fabricated at and below 30 nJ, multiphoton ionization is the dominant mechanism for structural modification. However, we could not observe structures below 30 nJ (except for PS) for PMMA and PDMS as the resolution of confocal microscope is nearly a micron. These calculations are done for our irradiation experiments carried out with 40X microscope objective with numerical aperture of 0.65. In case of LNB crystal also, tunneling ionization is the main dominant process though we have not shown in the graph its behavior almost resembles with these polymers.

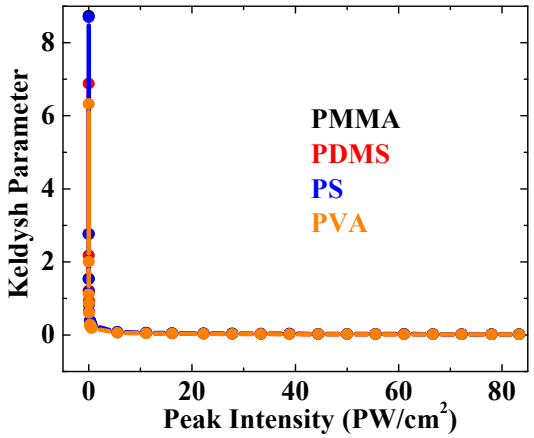

Figure 3. Keldysh parameter versus peak intensity for Polymers.

The availability of intensity to reach laser damage and minimal thermal effects presented above made researchers to use fs lasers for different applications. In our present study, we focus only on the formation of defects and hence higher energy pulses are used to fabricate the structures. Pristine polymers do not show emission in the visible region as their band gaps lie in the range of 3-7 eV [21]. These polymers are transparent to visible light. But upon irradiation with UV-visible or IR light, defects or optical centers and or free radicals are generated which exhibit luminescence behavior. Thus, one can fabricate micro features which are luminescent. Each luminescent micro feature can be treated as bit 1. Thus the fabricated micro craters find its applications in realizing the applications in memory based devices. Watanabe et al. have shown the luminescence through defect formation in vitreous silica [25] and Kudrius et al. have shown a similar effect in sapphire [26]. In both these cases, it is the formation of luminescent defects or optical centers that are responsible for the observation of photoluminescence behavior. However, such reports on the luminescence of fs laser irradiated polymers are sparse and yet to be explored and investigated.

Nie et al. reported multilayered optical bit memory in fluorescent Poly Methyl Meth Acrylate (PMMA) irradiated with fs pulses. Irradiated with fs laser the PMMA exhibited fluorescence when excited it at 442 nm which they attributed to the defects generated by bond scission. The excitation spectrum had a peak near 360 nm [27-29]. R. N. Nurmukhametov et al. [30] have exposed PS films and solutions with UV laser light beam (λ=248 nm) and observed changes in absorption and luminescent properties. They observed formation of optical centers with absorption band from 280-460 nm with fluorescence band from 330-520 nm. The absorption and emission spectra due to the fs laser irradiation in the present study match nearly with their reported work indicating the creation of similar optical centers. Thus there are reports in the literature that show observation of emission after treated with different irradiations. However, the origin of emission is still not pin pointed. In the present study, four polymers are investigated namely Poly Methyl Meth Acrylate (PMMA),

Poly Di Methyl Siloxane (PDMS), Poly Styrene (PS), and Poly Vinyl Alcohol (PVA). Photoluminescence is observed in all these cases when treated with fs laser irradiation [31-43]. Pure polymers have absorption in UV region. Hence, in order to modify these polymers, they have to be irradiated with UV light as Nurmukhametov et al. [30] have analyzed the spectra of solutions and thin films of polystyrene after treated with UV light. The investigations carried out by different groups show that the emission could be due to the formation of defects such as optical centers, the absorptions or excitations associated with the functional groups such as $n \rightarrow \pi^*$, $\pi \rightarrow \pi^*$ etc, which lead to emission and or due to photo selective excitation called the "Red Edge Effect". We focus on our investigations of emission in the irradiated regions of polymers below. Figure 4 shows one of the several structures fabricated in PS at 40 μJ energy with 40X (0.65 NA) objective lens. Pseudo green color shows emission when excited at 488 nm wavelength using confocal microscope. We obtained similar results even in case of other polymers also.

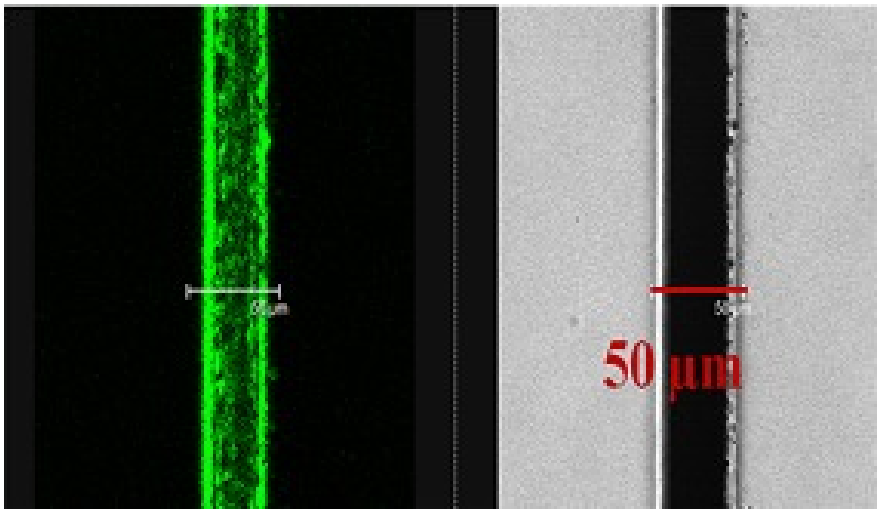

Figure 4. Confocal microscope image of a structure fabricated inside bulk PS [40 μJ energy, 1 mm/s speed, 50 μm width] Scale bar is 50 μm. Pseudo green color represents emission from the modified structure when excited at 488 nm wavelength.

Interestingly, we observed the shift in emission peak with excitation wavelengths. To study this phenomenon, we fabricated grating structures in polymers to increase effective area to capture fluorescence. In case of PMMA, we used energy 10 μJ, speed 1 mm/s, period 30 μm. In case of PDMS, PS and PVA we used energy of 50 μJ, speed 1 mm/s, period 10 μm; energy 1 μJ, speed 0.5 mm/s, period 30 μm; energy 10 μJ, speed 1mm/s, period 20 μm respectively. All these structures were fabricated using 40X with NA of 0.65 objective lens. Figure 5 (a) and (b) show the emission spectra recorded for PMMA excited from 200-560 nm. We clearly see the shift in the emission spectra with excitation wavelength. We observed similar effect even in case of other polymers irradiated with fs laser though the excitation spectra recorded look similar except PVA [31, 43].

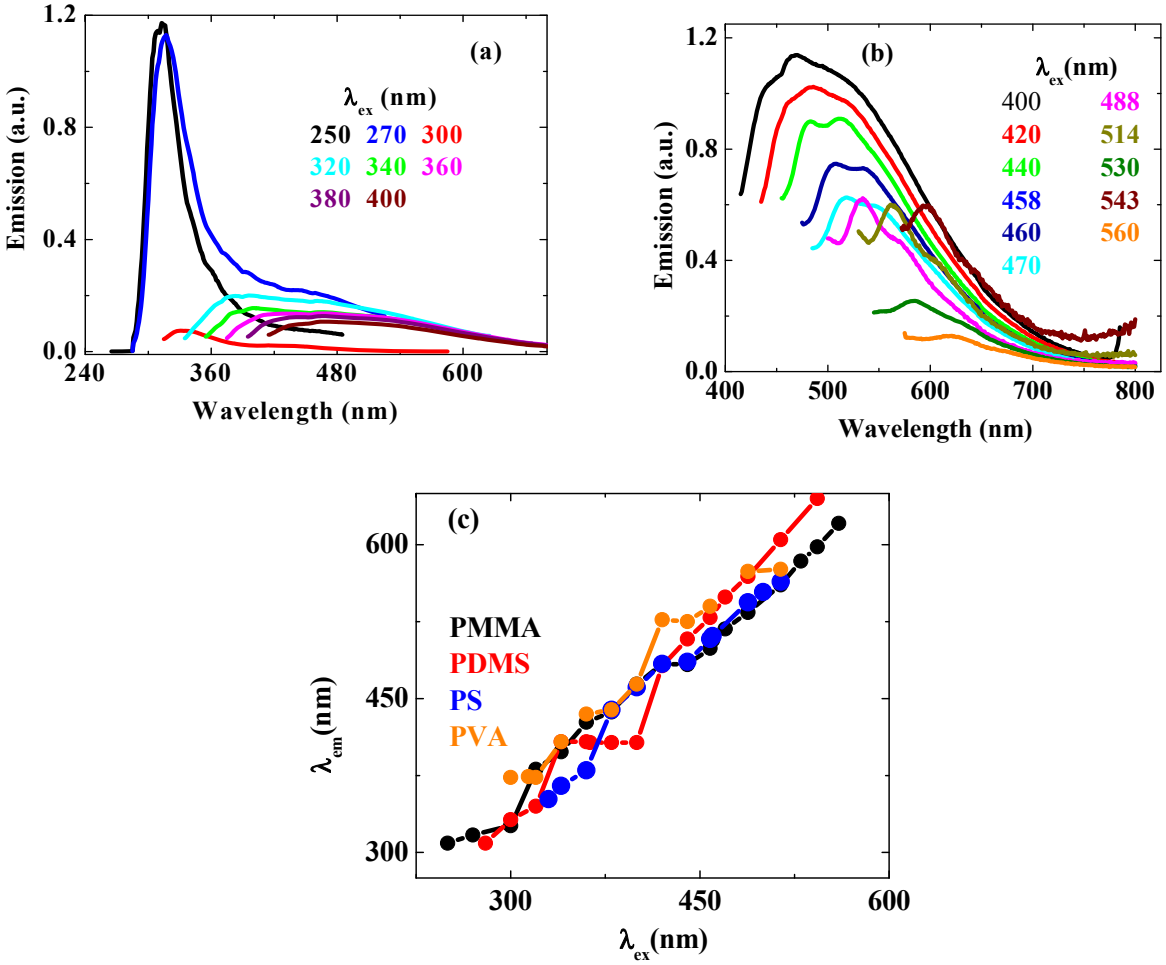

Figure 5. Plot of emission spectra of PMMA (a) at excitation wavelengths from 250-400 nm (b) at excitation wavelengths from 400-560 nm (c) Plot showing dependence of emission with excitation wavelength (Red edge effect).

The shift in emission peak with excitation wavelength is termed as red edge effect reported in the literature. Unusual spectroscopic behavior was reported earlier in case of organic fluorophores in rigid and highly viscous environments by W. Galley in Canada [44] and Rubinov in Belarus [45]. The unusual phenomena are the observation of the shift of fluorescence spectra with longer wavelengths of excitation that is red edge of the absorption spectrum in case of low temperature glasses. Varieties of fluorophores in different media with frozen or relatively slow structural dynamics from vitrified and highly viscous solutions to polymer matrices have shown similar effects. These phenomena did not account for concepts of independence of emission energy on excitation energy within the absorption band (Vavilov's law) and the occurrence of emission irrespective of excitation band, always from the lowest electronic and vibrational state of same multiplicity called Kasha's Rule [46-47].

These effects originate not from the violation of fundamental principles, but from their operation in specific conditions, when the ensemble of excited molecules is distributed in interaction energy with molecules in their surroundings. In a condensed medium, this distribution always exists at the time of excitation, but its display in a variety of spectroscopic phenomena depends on how fast the transitions are between the species forming this ensemble of states. Thus, REE is a site-selective effect which allows probing of the dynamics of redistribution of fluorophores between different environments [48]. The first observation of static REE in polymeric media were made with DMABN in PMMA and pyridine merocyanine dye in PVA [49-50]. REE effect was also reported in glassy polar polymer matrices [51], polymer

solutions [52], and hydrogels [53]. Excitation at the red edge results in the loss of vibrational structure and a shift to longer wavelength of fluorescence spectra, leaving the excitation spectra emission-independent.

In the present study, the fs laser irradiated polymers (whose details are explained above) have shown the REE as depicted in figure 5 (c). As these polymers contain functional groups like aldehyde, ketone etc., the maximum absorption bands can be attributed to transitions such as n $\rightarrow\pi^*$, $\pi \rightarrow\pi^*$ etc [54-56]. Also, we observed some of the bands matching with that of Raman. Since, the polymer medium is condensed; the resultant molecules after polymer chain scission due to irradiation may relax to one of the vibrational levels. In order to investigate the Raman and fluorescence bands, we calculated the Raman shift using the formula (6).

$$\Delta E(cm^{-1}) = \frac{1}{\lambda_{ex}} - \frac{1}{\lambda_{em}} \qquad (6)$$

where ΔE is wavenumber difference or Raman shift between excitation and emission wavelengths. λ_{ex} and λ_{em} are excitation and emission wavelengths respectively. For PMMA, the excitation wavelengths at 458, 488, 530, and 560 nm nearly match Raman mode of characteristic peak at 1736 cm^{-1} of γ (C=O) of (C-COO) mode [57]. Excitations at 380, and 400 nm nearly matched with Raman mode of 3454 cm^{-1} which is $2\gamma_2$ overtone of 1730 cm^{-1}. Excitation at 543 nm matched with another Raman peak of Combination band involving γ (C = C) and γ (C-COO) of PMMA which is at 1736 cm^{-1}. Our investigation extended to other polymers showed similar effects. Hence, we conclude that the origin of fluorescence from fs laser modified regions is due to REE, formation of optical centers (defects) and transitions matching the vibrational energies. In case of LNB crystal, we did not observe any emission and one of the reasons could be lack of functional or active group in the LNB crystalline media that give fluorescence upon irradiation.

Also, we have carried out ESR analysis to see further whether defects generated could be paramagnetic. Figure 6 (a) shows a microscope image of a fabricated grating structure on the surface of PS fabricated at 30 μJ energy, 1mm/s speed with 40 μm period. Figure 6 (b) shows a plot of ESR signal of fs laser irradiated PS (buried and surface) and pristine PS. From figure 6 (b), we clearly see that radical concentration of PS is almost negligible when grating is fabricated on the surface when compared with inside. Similar trend is observed in case of other polymers also. Also, we observed the ESR signal almost constant when ESR tube is oriented at different angles with respect to the magnetic field as depicted in figure 6 (c). Since these polymer materials are amorphous there is no symmetry present and ESR signal is independent of the orientation. Also the life time of free radicals generated in these polymers is nearly a day except in PDMS. From this we conclude that the defects (free radicals) responsible for ESR behavior are different from that causing emission as emission is observed even after one year. The radicals responsible are peroxide type of free radicals.

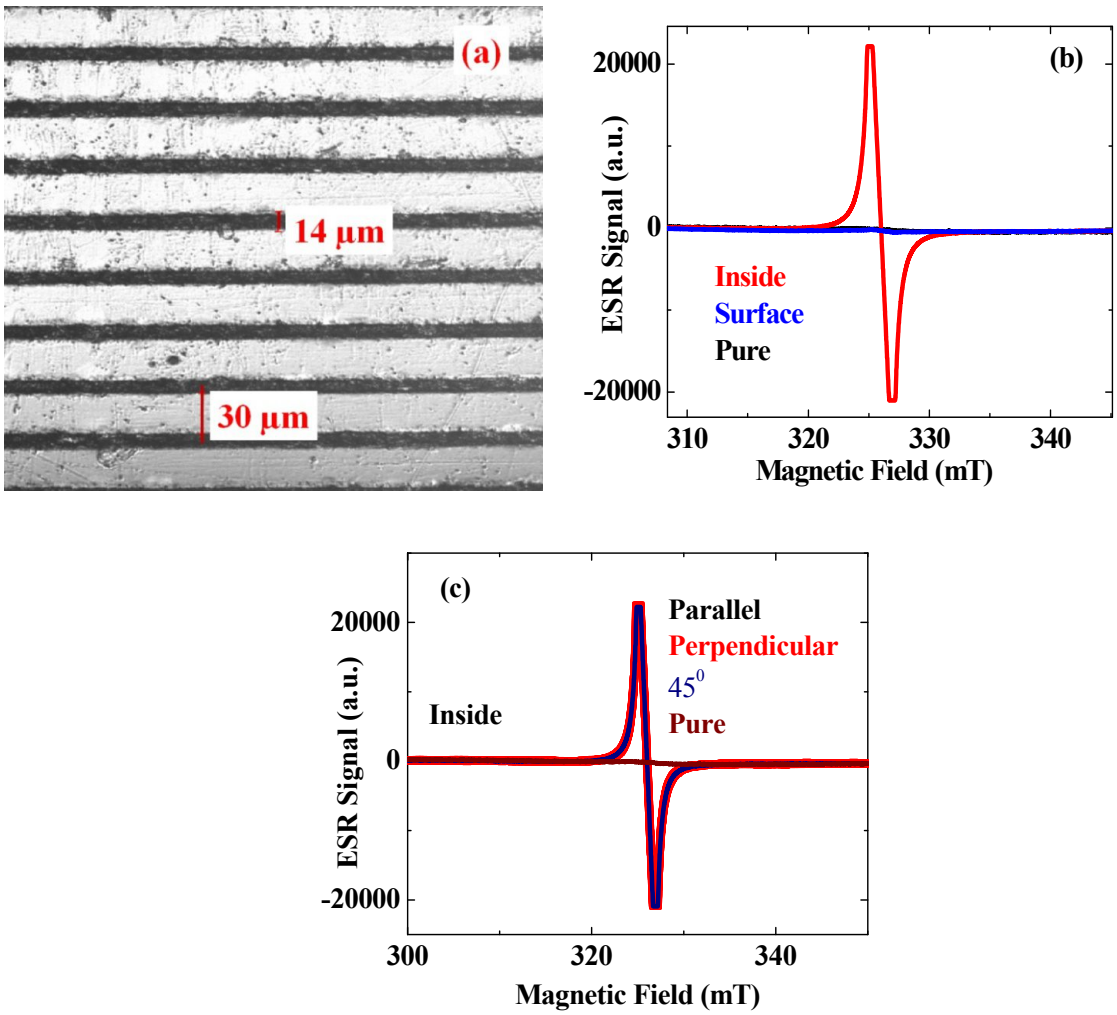

Figure 6. (a) Microscope image of a surface grating structure on PS (b) ESR signal of fs irradiated PS a pristine PS (c) ESR signal with orientation of sample.

To carry out ESR analysis, we fabricated gratings underneath and on the surface of the lithium niobate crystal. Energy used was 100 µJ with 40 X microscope objective and 1 mm/s as the scanning speed. Grating structure has 20 µm period. In case of polymers we observed paramagnetic radicals in all orientations of the sample with respect to the direction of magnetic field (Parallel, Perpendicular and 45°). Since the properties of the crystals are anisotropic due to symmetry involved in the crystal structure, we observed orientation dependent ESR signal. Interestingly, pristine LNB crystal has also shown ESR signal when sample was oriented parallel to the magnetic field direction. Figure 7 (a) shows the ESR signals in three different orientations of the crystal with respect to the direction of magnetic field applied. Only parallel orientation of the crystal with respect to the magnetic field has shown the existence of paramagnetic radicals. Figure 7 (b) shows the results obtained with irradiated sample (for buried grating). Similar results were obtained, since the irradiated crystal also contains maximum volume of pure crystal, It has exhibited ESR signal in parallel configuration. Figure 7 (c) compares ESR signals of irradiated and unirradiated samples in parallel configuration. Thus, we conclude that there are no free radicals generated through irradiation process in LNB crystal unlike polymer media.

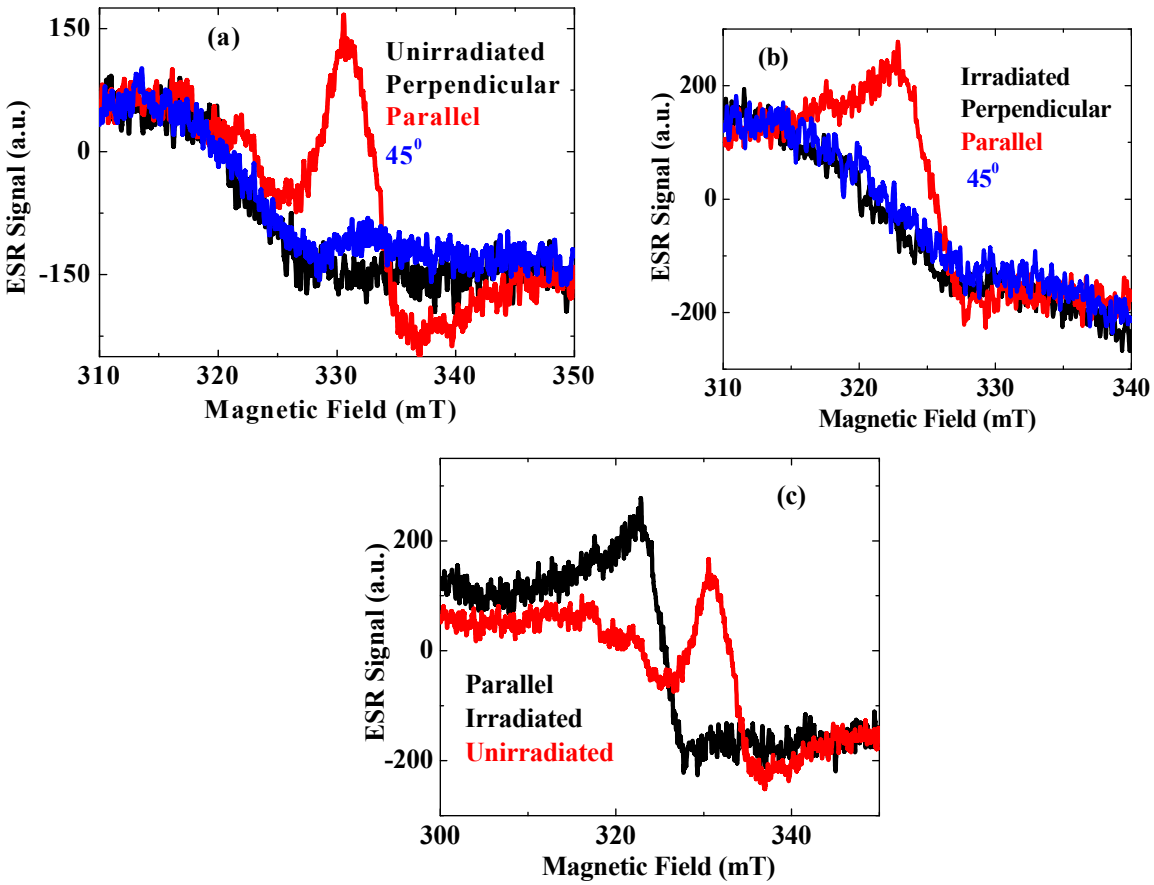

Figure 7. ESR signal of (a) Unirradiated pure LNB crystal in different orientations (b) Unirradiated pure LNB crystal in different orientations (c) Irradiated and pure crystals in parallel orientation.

We investigated the fs laser modified regions of polymers and LNB crystal. We observed broadening and suppression of Raman modes in case of polymers which indicated us the formation of defect states described above [32-35, 41-43]. Figure 8 (a) and 8 (b) show the Raman analysis carried out at higher and lower energies of writing with 40X (0.65 NA) microscope objective lens. We clearly see the broadening effects at higher fluences of writing. Table 3 shows the assignment of Raman modes of PVA [58-59].

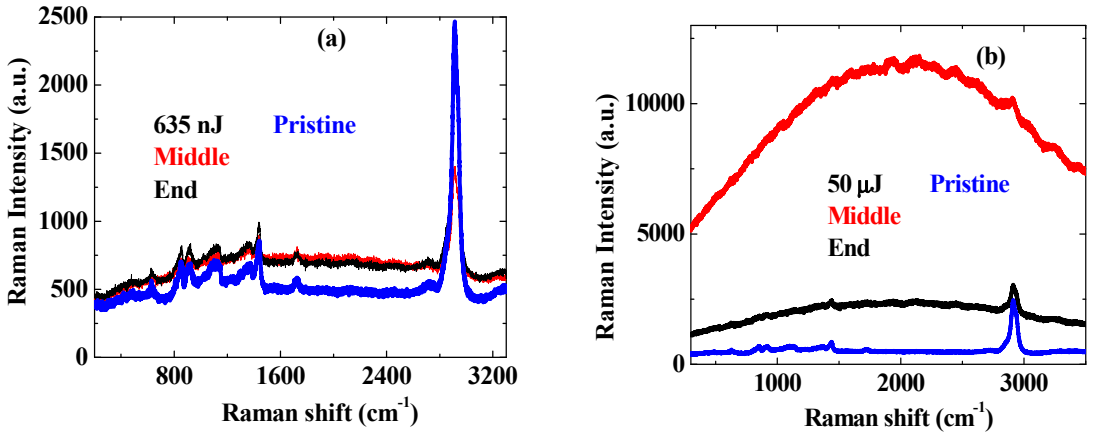

Figure 8. (a) Raman spectra of a structure fabricated in PVA thin film at 635 nJ energy, 1 mm/s speed (b) Raman spectra of a structure fabricated in PVA thin film at 50 µJ energy, 1 mm/s speed.

Table 3. The assignment of different Raman modes.

S. No.	Raman shift (cm^{-1})	Assignment
1	310	C-C torsion and bending
2	410	γ_w(C-O)
3	477	δ(C-O) CH out of plane
4	563	γ_w(OH), CH out of plane
5	856	γ(C-C)
6	918	γ(C-C)
7	1095	γ(C-O)
8	1145	γ(C-O), γ(C-C)
9	1232	γ_w(CH)
10	1356	γ_w(CH2), δ(OH)
11	1440	δ(CH2), δ(OH)
12	1710	γ(C=O) Residual acetate
13	2721	γ(CH) weak band
14	2910	γ(CH) of CH_2

We fabricated several structures in LNB crystal and carried out Raman analysis. Figure 9 (a) shows the Raman modes of LNB crystal. We collected Raman spectra for a structure fabricated at 100 µJ energy in middle and end regions and also for a structure fabricated at 40 µJ energy with 0.5 mm/s scanning speed and using 40X objective. In case of LNB crystal, we did not observe any changes in Raman peaks except change in intensity which could be due to lattice deformity leading to creation of defects [60-68].

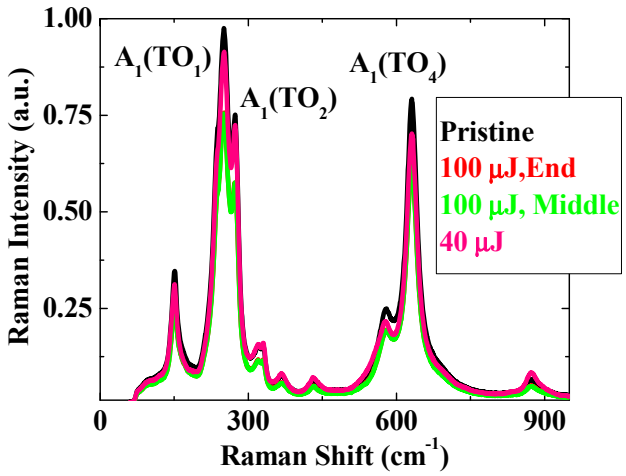

Figure 9. Raman analysis of fabricated structures in LNB crystal.

4. CONCLUSIONS

In our spectroscopic investigation on fs laser irradiated polymers compared with LNB crystal, we presented defect generation in these two media. Polymers exhibited emission after irradiation and showed red edge effect due to its condensed phase. The origin of emission is due to formation of optical centers (as polymers have functional groups) due to polymer chain scission and sometimes overlapping of Raman modes. Polymers showed the presence of peroxide type free radicals though these radicals are not responsible for emission. LNB crystal did not show any of these effects. Further investigations through confocal micro-Raman studies indicated and confirmed the presence of defects in polymers and lattice deformities in LNB crystal.

ACKNOWLEDGEMENTS

KLND acknowledges CSIR for his financial support.

REFERENCES

1. Schaffer, C.B., Brodeur, A, Garcia, J. F., Mazur, E., "Micromachining bulk glass by use of femtosecond laser pulses with nanojoule energy," Opt. Lett. 26**,** 93-95 (2001).
2. Gattass, R. R., Mazur, E., "Femtosecond laser micromachining in transparent materials," Nat. Phot. 2, 219-225 (2008).
3. Perry, M. D., Stuart, B. C., Banks, P. S., Feit, M. D., Yanovsky, V., Rubenchik, A. M., "Ultrashort-pulse laser machining of dielectric materials," J. Appl. Phys. 85, 6803-6810 (1999).
4. Sundaram, S. K., Mazur, E., "Inducing and probing non-thermal transitions in semiconductors using femtosecond laser pulses," Nat. Mater. 1, 217-224 (2002).
5. Chichkov, B. N., Momma, C., Nolte, S., Von Alvensleben, F., Tunnermann, A., "Femtosecond, picosecond and nanosecond laser ablation of solids," App. Phys. A 63, 109-115 (1996).
6. Gamaly, E. G., Rode, A. V., Luther-Davies, B., Tikhonchuk, V. T., "Ablation of solids by femtosecond lasers: Ablation mechanism and ablation thresholds for metals and dielectrics," Phys. Plasmas 9, 949-957 (2002).
7. Hallo, L., Bourgeade, A., Tikhonchuk, V. T., Mezel, C., Breil, J., "Model and numerical simulations of the propagation and absorption of a short laser pulse in a transparent dielectric material: blast-wave launch and cavity formation," Phys. Rev. B 76, 024101 (2007).
8. Keldysh, L.V. "Ionization in the field of a strong electromagnetic wave," Sov. Phys. JETP **20**, 1307 (1965).
9. Boyd, R.W., "Nonlinear Optics," 3rd edition, Academic Press, 1992.

10. Baum, A., Scully, P. J., Perrie, W., Jones, D., Issac, R., Jaroszynski, D. A., "Pulse-duration dependency of femtosecond laser refractive index modification in poly(methyl methacrylate)," Opt. Lett. 33, 651-653 (2008).
11. Singh, L., Samra, K. S., "Opto-structural characterization of proton (3 MeV) irradiated polycarbonate and polystyrene,"Rad. Phys. Chem. 77, 252 (2008).
12. Mathad, R. D., Harish Kumar, H. G., Sannakki, B., Ganesh, S., Sarma, K. S. S., Badiger, M. V., "High energy electron irradiation effects on polystyrene films," Radiation Effects & Defects in Solids 164 (10), 656–664 (2009).
13. Jabbar, W.A., Habubi, N.F., Chiad, S.S., "Optical Characterization of Silver Doped Poly (Vinyl Alcohol) Films," J. Arkansas Acad. Sci., 64, 101-105 (2010).
14. Lovinger, A.J., Davis, D.D., Schilling, F.C., Padden, Jr., F.J., Bovey, F.A., Zeiglert, J.M. "Solid-state Structure and Phase Transitions of Poly (dimethylsilylene), Macromolecules," 24, 132-139 (1991).
15. Christensen, F. K., Mullenborn, M., "Sub-band-gap laser micromachining of lithium niobate," Appl. Phys. Lett. 66 (21), 2772-2773 (1995).
16. Thierfelder, C., Sanna, S., Arno Schindlmayr, Schmidt, M. G., "Do we know the bandgap of lithium niobate," Phys. status Solidi C 7, No. 2, 362-365 (2010).
17. Hung, W.S.Y, Chen, C.S., Haviland, J.K. "Further Analytical Study of Hybrid Rocket Combustion," Report # NASA-CR-112201 AEEP-4041-106-72U, 1972.
18. Karabeyoglu, M. A., Altman, D., and Bershader, D., "Transient Combustion in Hybrid Rockets," AIAA Paper 95-2691, July 1995.
19. Muzzy, R.J., Wooldridge, C.E. "Internal Ballistic Considerations in Hybrid Rocket Design," J. Spacecraft, 4(2), 255-262, (1967). doi: 10.2514/3.28844
20. Tleoubaev, A., Brzezinski, A. "Thermal Diffusivity and Volumetric Specific Heat Measurements Using Heat Flow Meter Instruments for Thermal Conductivity 29 / Thermal Expansion 17 Conference, Laser Comp, Inc., 20 Spring Street, Saugus, Massachusetts 01906 USA. http://www.lasercomp.com/Tech%20Papers/Papers/Thermal%20Diffusivity%20and%20Volumetric%20Specific%20Heat%20Measurements%20Using%20Heat%20Flow%20Meter%20Instruments.pdf
21. Gamaly, E. G., Juodkazis, S., Nishimura, K., Misawa, H., Luther-Davies, B., Hallo, L., Nicolai, P., Tikhonchuk, V. T., "Laser-matter interaction in the bulk of a transparent solid: Confined microexplosion and void formation," Phys. Rev. B 73, 214101 (2006).
22. Stuart, B. C., Feit, M. D., Herman, S., Rubenchik, A. M., Shore, B. W., Perry, M. D., "Nanosecond-to-Femtosecond Laser-Induced Breakdown in Dielectrics," Phys. Rev. B 53, 1749-1761(1996).
23. Tien, A. C., Backus, S., Kapteyn, H., Murnane, M., Mourou, G., "Short-Pulse Laser Damage in Transparent Materials as a Function of Pulse Duration," Phys. Rev. Lett. 82, 3883-3886 (1999).
24. Sanner, N., Uteza, O., Chimier, B., Sentis, M., Lassonde, P., Legare, F., Kieffer, J. C., "Toward determinism in surface damaging of dielectrics using few-cycle laser pulses," Appl. Phys. Lett. 96, 071111 (2010).
25. Watanabe, M., Juodkazis, S., Sun, H. B., Matsuo, S., Misawa, H., "Luminescence and defect formation by visible and near-infrared irradiation of vitreous silica," Phys. Rev. B 60, 9959 (1999).
26. Kudrius, T., Slekys, G., Juodkazis, S., "Surface-texturing of sapphire by femtosecond laser pulses for photonic applications," J. Phys. D: Appl. Phys. 43, 14550 (2010).
27. Nie, Z. Lee, H., Yoo, H., Lee, Y., Kim, Y., Lim, K. S., Lee, M., "Multilayered optical bit memory with a high signal-to-noise ratio in fluorescent polymethylmethacrylate,"Appl. Phys. Lett. 94, 111912 (3 pages) (2009).
28. Nie, Z., Lim, K. S., Lee, H., Lee, M., Kabayashi, T., "Femtosecond laser induced photoluminescence in poly (methyl methacrylate) and three-dimensional optical storage," J. Lumin.131, 266-270 (2011).
29. Nie, Z. G., Lim, K. S., Jang, W. Y., Lee, H. Y., Lee, M. K., Kabayashi, T., "Multilayered optical bit storage in $Sm(DBM)_3Phen$-doped poly(methyl methacrylate) read out by fluorescence and reflection modes," J. Phys. D: Appl. Phys. 43, 485101 (6 pages) (2010).
30. Nurmukhametov, R. N., Volkova, L. V., Kabanov, S. P., "Fluorescence and absorption of polystyrene exposed to UV laser radiation," J. Appl. Spectr. 73, 55-60 (2006).
31. Deepak, K. L. N., Kuladeep, R., Venugopal Rao, S., Narayana Rao, D., "Luminescent microstructures in bulk and thin films of PMMA, PDMS, PVA, and PS fabricated using femtosecond direct writing technique," Chem. Phys. Lett. 503, 57-60 (2011).
32. Deepak, K. L. N., Narayana Rao, D., Venugopal Rao, S., "Fabrication and Optical Characterization of microstructures in PMMA and PDMS using femtosecond pulses for photonic and micro fluidic applications," Appl. Opt. 49(13), 2475-2489 (2009).

33. Deepak, K. L. N., Narayana Rao, D., Venugopal Rao, S., "Femtosecond Laser Written Microstructures in PDMS and PMMA for Photonic Applications," ICALEO 2009*-28th International Congress on Applications of Lasers and Electro-Optics, Congress Proceedings* 102 , 1499-1506 (2009). (**ISBN:** 978-0-912035-59-8).
34. Deepak, K. L. N., Kuladeep, R., Narayana Rao, D., "Emission properties of femtosecond (fs) laser fabricated microstructures in Polystyrene (PS)" Opt. Commun. 284, 3070-3073 (2011).
35. Deepak, K. L. N., Kuladeep, R., Praveen Kumar, V., Venugopal Rao, S., Narayana Rao, D., "Spectroscopic investigations of femtosecond laser irradiated Polystyrene and fabrication of microstructures," Opt. Commun. 284, 3074-3078 (2011).
36. Deepak, K. L. N., Venugopal Rao, S., Narayana Rao, D., Effect of heat treatment to efficient buried diffraction gratings in Polystyrene" Appl. Surf. Sci. **257**, 9299-9305 (2011).
37. Deepak, K. L. N., Kuladeep, R., Venugopal Rao, S., Narayana Rao, D., "Studies on Defect Formation in Femtosecond Laser Irradiated PMMA and PDMS," Radiation Effects and Defects in Solids **167(2)**, 88-101 (2012).
38. Deepak, K. L. N., Venugopal Rao, S., Narayana Rao, D., "Femtosecond laser-fabricated microstructures in bulk poly(methylmethacrylate) and poly(dimethylsiloxane) at 800 nm towards lab-on-a-chip applications," Pramana **75 (6)**, 1221-1232 (2010).
39. Deepak, K. L. N., Venugopal Rao, S., Narayana Rao, D., "Femtosecond laser microfabrication in polymers towards memory devices and microfluidic applications" Proc. SPIE, 8190, 81900R1, 2011.
40. Venugopal Rao, S., Turaga, S.P., Deepak K. L. N., Tewari, S.P., Gundawar, M.K, Desai, N.R. "Laser direct writing of photonic structures in X-cut lithium niobate using femtosecond pulses" Proc. SPIE, 8173, 81730G1 (8 pages) 2010.
41. Deepak, K. L. N., Venugopal Rao, S., Narayana Rao, D., "Femtosecond Laser Direct Writing and Spectroscopic Characterization of Microstructures, Craters, and Gratings in Bulk/Thin Films of Polystyrene," AIP Conf. Proceedings 1391, 271-274 (2011).
42. Deepak**,** K. L. N., Venugopal Rao, S., Narayana Rao D., "Femtosecond laser direct writing in polymers and potential applications in microfluidics and memory devices," Opt. Eng. 51, 073402 (6 pages) (2012).
43. Deepak, K.L.N., Venugopal Rao, S., Narayana Rao, D. "Direct Writing in Polymers with Femtosecond Laser Pulses: Physics and Applications," Laser Pulses, Ed. Prof. Dr. Igor Peshko, InTech Publishers, Croatia, pp. 277-294, 2012. ISBN 979-953-307-845-7
44. Galley, W.C. and Purkey, R.M., "Role of heterogeneity of the solvation site in electronic spectra in solution," Proc. Natl Acad. Sci. USA 67, 1116-1121 (1970).
45. Rubinov, A. N. and Tomin, V.I., "Bathochromic luminescence of organic dyes," Opt. Spektr. 29(6), 1082-1086 (1970).
46. Terenin, A.N., "Photonics of dye molecules and allied organic compounds," Nauka, Leningrad, 616p. 1967 (Russian). http://www.niif.spbu.ru/departments/chem-ph/Gallery/terenin.htm
47. Birks, J.B., "Photophysics of Aromatic molecules," Wiley-Inter-science, London, 1970.
48. Alexander P. Demchenko, "The red-edge effects: 30 years of exploration," Luminescence, 17, 19-42 (2002).
49. Al-Hassan KA and Rttig W, "Free volume sensing fluorescent probes, Chem. Phys. Lett. 268, 110-116 (1997).
50. Al-Hassan K. A., El-Bayoumi M. A. , "Large edge-excitation red shift for a merocyanine dye in poly (vinyl alcohol) polymer matrix," J. Polymer Sci. B 25, 495-500 (1987).
51. Al-Hassan K. A., Azumi T. , "The red edge effect as a tool for investigating the origin of the anomalous fluorescence band of 9,9'-bianthryl in rigid polar polymer matrices," Chem. Phys. Lett. 150, 344-348 (1988).
52. Bajorek A., Paczkowski J., "Influence of the attachment of chromophores to a polymer chain on their twisted intramolecular charge transfer in dilute solution," Macromolecules 31, 86-95 (1998).
53. Datta A, Das S, Mandal D, Pal S. K., Bhattacharyya K., "Fluorescence monitoring of polyacrylamide hydrogel using 4-aminophthalimide," Langmuir 13, 6922-6926 (1997).
54. Talapatra, G.B., Narayana Rao, D., Prasad, P. N., "spectal diffusion within the inhomogeneously broadened- n-π^* singlet-triplet transition of the orientationally disorder solid of 4-bromo-4-chlorobenzophenone," J. Phys. Chem. 8(20), 4636-4640 (1984).
55. Xu, J., Huang, X.H., Zhou, N.L., Zhang, J.S., Bao, J.Ch., Lu, T.H. , Li, C., "Synthesis, XPS and fluorescence properties of Eu^{3+} complex with polydimethylsiloxane," Mat. Lett. 58, 1938–1942 (2004).
56. Banwell, C.N, McCash, E.M., "Fundamentals of Molecular Spectroscopy," 4th edition, Tata McGraw-Hill, New Delhi, 1995.

57. Thomas, K. J., Sheeba, M., Nampoori, V. P. N., Vallabhan, C. P.G., Radhakrishnan, P., "Raman spectra of polymethyl methacrylate optical fibres excited by a 532 nm diode pumped solid state laser," J. Opt. A: Pure Appl. Opt. 10, 055303 (5pp) (2008).
58. Badr, Y., Mahmoud, M. A., "Enhancement of the Optical Properties of Poly Vinyl Alcohol by Doping with Silver Nanoparticles," Journal of Applied Polymer Science 99, 3608–3614 (2006).
59. Ashcroft, N.W., Mermin, N.D., "Solid State Physics," Holt Rinehart and Winston, New York, 1976.
60. Rodenas, A., Nejadmalayeri, A.H., Jaque, D., Herman, P. "Confocal Raman mapping of optical waveguides in $LiNbO_3$ fabricated by ultrafast high-repetition rate laser-writing," Opt. Exp. 16, 13979-13989 (2008).
61. Burghoff, J., Hartung, H., Nolte, S., Tunnermann, A., "Structural properties of femtosecond laser-induced modifications in $LiNbO_3$," Appl. Phys. A 86, 165-170 (2007).
62. Caciuc, V., Postnikov, A. V., Borstel, G., "Ab initio structure and zone-center phonons in $LiNbO_3$," Phys. Rev. B 61 (13), 8806-8813 (2000).
63. Kostritskii, S. M., Moretti, P., "Micro-Raman study of defect structure and phonon spectrum of He-ion implanted LiNbO3 waveguides," Phys. Stat. Sol (c) 1(11), 3126-3129 (2004).
64. Zhang, Y., Guilbert, L., Bourson, P., Polgar, K., Fontana, M. D., "Characterization of short range heterogeneties in sub-congruent lithium niobate by micro-Raman spectroscopy," J. Phys. Cond. Matter. 18, 957-963 (2006).
65. Abdi, F., Aillerie, M., Bourson,P., Fontana, M. D., Polgar, K., "Electro-optic properties in pure $LiNbO_3$ crystals from the congruent to the stoichiometric composition," J. Appl. Phys. 84, 2251-2254 (1998).
66. Jayaraman, A., Ballman, A. A., "Effect of pressure on the Raman modes in $LiNbO_3$ and $LiTaO_3$," J. Appl. Phys. 60, 1208-1212 (1986).
67. Merchant, C. A., Aitchison, J. S., GarciaBlanco, S., Hnatovsky, C., Taylor, R. S., Agullo F., Rueda, Kellok, A. J., Baglin, J. E. E., "Direct observation of waveguide formation in KGd(WO4)2 by low dose H+ ion implantation," Appl. Phys. Lett. 89, 111116 (3 pages) (2006).
68. Savova, I. Savatinova, Liarokapis, E., "Phase composition of z-cut protonated $LiNbO_3$:a Raman study," Opt. Mat. 16, 353-360 (2001).

(8530-3)
"Spectroscopic investigation of fs laser-induced defects in polymer and crystal media"
853004
Questions and Answers

Q. What was the ambient condition for your processing? Did you do it in air or in any kind of vacuum chamber?

A. No, it's in air, because most of the time we are subsurface. Most of the channels are written in the subsurface so actually the ambient medium does not matter. It's done inside of the polymer matrix.